

The pyrolytic decomposition of synthetic violarites of various stoichiometry

A.C. Chamberlain^{a,*}, J.G. Dunn^b

^a *WMC Resources Ltd., Mineral Processing Group, Nickel Division, Belmont, Western Australia 6104, Australia*

^b *School of Applied Chemistry, Curtin University of Technology, Perth, Western Australia, Australia*

Received 10 September 1997; accepted 23 January 1998

Abstract

Four samples of violarite of different stoichiometry were synthesised and characterised. The pyrolytic decomposition of $\text{Fe}_{0.97\pm 0.01}\text{Ni}_{1.96\pm 0.02}\text{S}_{4.0\pm 0.03}$ of particle size 45–63 μm was examined at a heating rate of $10^\circ\text{C min}^{-1}$ in a nitrogen atmosphere using a simultaneous thermogravimetric–differential thermal analyser (TG-DTA). The first reaction observed was the loss of sulfur between 420° and 525°C , giving a mass loss of 2.25% with the formation of a monosulfide solid solution (mss), violarite of a different stoichiometry, and a minor amount of vaesite. An endothermic peak at 495°C was assigned to a phase transition from a thiospinel structure to mss. Further sulfur losses of 7.65 and 4.10% took place in the 525 – 615°C and 615 – 795°C ranges, and the products were mss of increasing metal richness, with $(\text{Fe,Ni})_{3\pm x}\text{S}_2$ also existing in the higher temperature range. This last phase melted at 835°C . Finally, more sulfur was lost between 845° and 900°C from the molten material. Products were taken at different temperatures for characterisation by X-ray diffraction (XRD), scanning electron microscopy (SEM), and electron probe microanalysis (EPMA). The TG-DTA curves for all four samples were obtained under similar conditions. The samples were all found to decompose by the same reaction sequence. The endothermic events associated with the thiospinel transition, and the melting of $(\text{Fe,Ni})_{3\pm x}\text{S}_2$, shifted to lower temperatures as the nickel concentration of the original violarite increased. © 1998 Elsevier Science B.V.

Keywords: Pyrolytic decomposition; Mechanism of decomposition; Stoichiometry; Nickel sulphide; Violarite

1. Introduction

Violarite, of stoichiometric formula FeNi_2S_4 , is a nickel-bearing mineral that is a major source of feed-stock in the production of nickel metal. It is commonly found as a secondary mineral formed by the supergene alteration of other minerals such as pentlandite $(\text{Fe,Ni})_9\text{S}_8$ [1]. Violarite deposits exhibit a wide range of compositions, which cover the solid-solution series from violarite to polydymite (Ni_3S_4) [2], and are often sulphur-deficient relative to the ideal metal : sulphur

ratio of 3 : 4 [3]. Violarites which coexist with millerite (NiS) or vaesite (NiS_2) tend to be nickel-rich, whilst violarites that coexist with pyrite-millerite assemblages vary between iron-rich polydymite and cobalt-rich violarite [4].

One of the difficulties with investigating violarite is that its properties are very similar to many other sulphide minerals with which it coexists. Hence, the isolation of violarite from commonly associated sulphide minerals is very difficult. On the other hand, violarites of various compositions can be synthesised in the laboratory. This requires a two-step process, the first one involving the reaction of Ni, Fe and S to form

*Corresponding author.

a monosulphide solid solution (mss) of formula $(\text{Fe,Ni})_{1-x}\text{S}$, followed by reaction with additional sulphur to achieve a 3 : 4 metal : sulphur ratio [5] [6]. We have used this method to prepare four violarites in the solid solution range, and used them to study the mechanism of their pyrolytic decomposition. Samples were heated at $10^\circ\text{C min}^{-1}$ in a nitrogen atmosphere using simultaneous TG-DTA, and products collected at various temperatures for characterisation and examination of the particle morphology.

2. Experimental

2.1. Synthesis of violarite samples

Iron, nickel and sulphur of >99.99% purity were obtained from Aldrich.

A typical experiment required, firstly, the synthesis of mss containing iron and nickel to give the desired iron : nickel ratio. The required amounts of iron, nickel and sulphur were weighed accurately, mixed and sealed in a Vycor[®] tube under a vacuum of 0.01013 kPa. The tube was heated to 130–140°C for 15 min in a furnace, and then the temperature increased to 700°C. After 24 h, the tube was removed and rapidly quenched in ice water. The mss sample was removed and ground to <45 μm in an agate mortar and pestle under acetone. The ground sample was placed in a clean tube with a piece of Vycor[®] rod to reduce the volume of dead space and the contents sealed under vacuum. The tube was heated to 700°C for 48 h. This process was repeated again for another 48 h at 700°C.

The final homogeneous mss phase was reground and the quantity of sulphur required to give the final stoichiometry added to the mss. The mixture was placed in a tube with a length of Vycor[®] rod inside

and sealed under vacuum, and heated to $300\pm 1^\circ\text{C}$ for 10 days. The sample was quenched in ice water and ground to <45 μm , and the ground sample resealed under vacuum and heated to $300\pm 1^\circ\text{C}$ for 20 days. The reaction tube was rapidly quenched in ice water and the resulting homogeneous violarite stored in dry nitrogen.

2.2. Characterisation of violarite samples

The percentage iron, nickel and sulphur in each sample was determined using classical wet chemical techniques. Each analysis was carried out in duplicate, and the results are given in Table 1.

XRD analysis detected violarite as the only phase present. The particle size chosen for the experimental programme was 45–63 μm .

2.3. Equipment and procedures

XRD patterns were acquired using a Siemens D500 diffractometer. SEM was performed using a JEOL JSM-6400 scanning electron. EPMA data was collected from carbon-coated polished sections using a Cameca SX-50 electron probe. Pyrite and nickel metal were used as standards for quantitative analysis.

TG-DTA measurements were performed using a Stanton–Redcroft thermal analyser STA-781. All experiments were carried out in alumina crucibles measuring 4 mm in diameter and 5 mm deep. Thereafter, 5 mg samples were heated at $10^\circ\text{C min}^{-1}$ in nitrogen flowing at 40 ml min^{-1} .

3. Results and discussion

Fig. 1 shows a typical TG-DTA curve for $\text{Fe}_{0.97}\text{Ni}_{1.96}\text{S}_4$ heated at $10^\circ\text{C min}^{-1}$ in nitrogen. There

Table 1
Results of wet chemical analysis of the four synthetic violarites

Sample	Average composition (wt%)				Stoichiometry
	Fe	Ni	S	total	
1	18.24	38.66	43.34	100.24	$\text{Fe}_{0.97\pm 0.01}\text{Ni}_{1.96\pm 0.02}\text{S}_{4.0\pm 0.03}$
2	13.54	43.98	44.19	101.71	$\text{Fe}_{0.73\pm 0.01}\text{Ni}_{2.26\pm 0.02}\text{S}_{4.0\pm 0.03}$
3	8.59	48.69	43.98	101.26	$\text{Fe}_{0.46\pm 0.01}\text{Ni}_{2.49\pm 0.02}\text{S}_{4.0\pm 0.03}$
4	3.74	53.32	43.39	100.45	$\text{Fe}_{0.20\pm 0.01}\text{Ni}_{2.72\pm 0.02}\text{S}_{4.0\pm 0.03}$

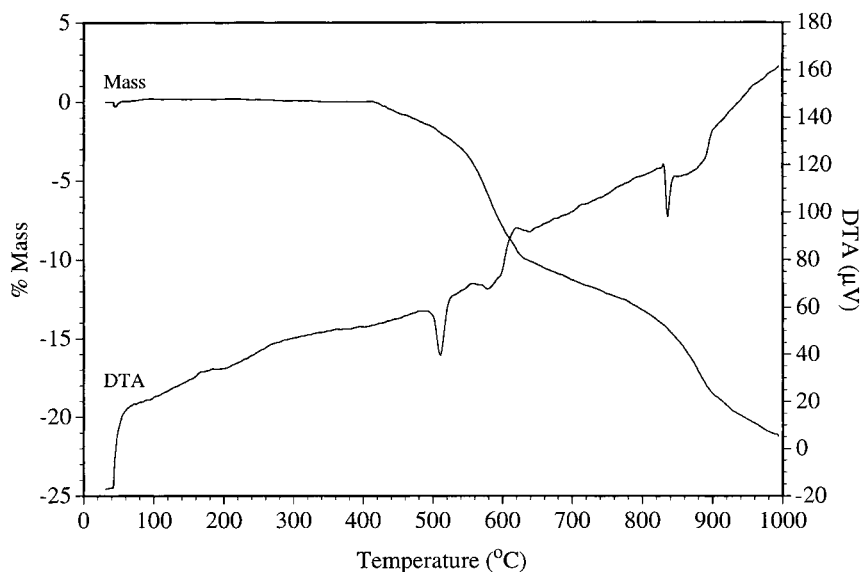


Fig. 1. Typical TG-DTA trace of $\text{Fe}_{0.97}\text{Ni}_{1.96}\text{S}_4$ heated at $10^\circ\text{C min}^{-1}$ in a nitrogen atmosphere.

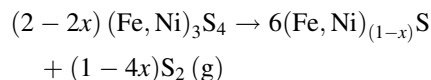
was no TG-DTA activity observed prior to 420°C . Micrographs of polished samples collected between $385\text{--}420^\circ\text{C}$ showed no evidence of pyrolytic decomposition. Quantitative EPMA across the particles gave the same results as those obtained for the unreacted sample.

Pyrolytic decomposition commenced above 420°C , with a small mass loss of 2.25% observed between $420\text{--}525^\circ\text{C}$. Analysis by XRD of samples collected at 425°C revealed violarite as the major phase with a minor trace of mss present (Fig. 2). SEM micrographs taken of a sample collected at 425°C showed small ragged regions of mss within the violarite host (Fig. 3(a)), as well as the presence of a small amount of vaesite, $(\text{Ni,Fe})\text{S}_2$. When analysed by EPMA, violarite and mss had an average composition of $\text{Fe}_{1.14}\text{Ni}_{1.86}\text{S}_{3.86}$ and $\text{Fe}_{0.36}\text{Ni}_{0.56}\text{S}_{1.00}$, respectively. The EPMA results showed an increase in the iron : nickel ratio for both violarite and mss compared to the initial violarite starting material.

By 490°C , mss and violarite were identified as the major phases in the XRD pattern along with a minor amount of vaesite (Fig. 2). SEM examination of the violarite sample still showed a significant portion of violarite remaining with an increase in the amount of mss as the next major phase (Fig. 3(b)). A minor amount of vaesite was also detected. There was no

evidence of vaesite found in association with violarite. In all cases, the vaesite was exsolved within the mss phase. A small porous outer rim, $\approx 2\ \mu\text{m}$ thick, was evident around the majority of the particles, probably caused by the evolution of sulphur vapour from the surface of the particle. EPMA results of the violarite and mss at 490°C showed a large decrease in the sulphur concentration. Approximately 20 particles were analysed for each phase present. The sulphur concentration was significantly lower for the mss phase compared with the composition found at 425°C , with the composition approaching a 1 : 1 metal : sulphur ratio. The mean composition of the violarite host was $\text{Fe}_{1.15}\text{Ni}_{1.85}\text{S}_{3.87}$, whereas the mss had a mean stoichiometry of $\text{Fe}_{0.38}\text{Ni}_{0.54}\text{S}_{1.00}$. The violarite still exhibited a cubic thiospinel crystal structure despite having lost a minor amount of sulphur from its lattice.

Hence, the evolution of sulphur gas from the violarite lattice resulting in the formation of mss would account for the small mass loss between 420° and 525°C , as represented by the following reaction:



At 495°C , a sharp endothermic peak was observed in the DTA trace with an onset and offset temperature

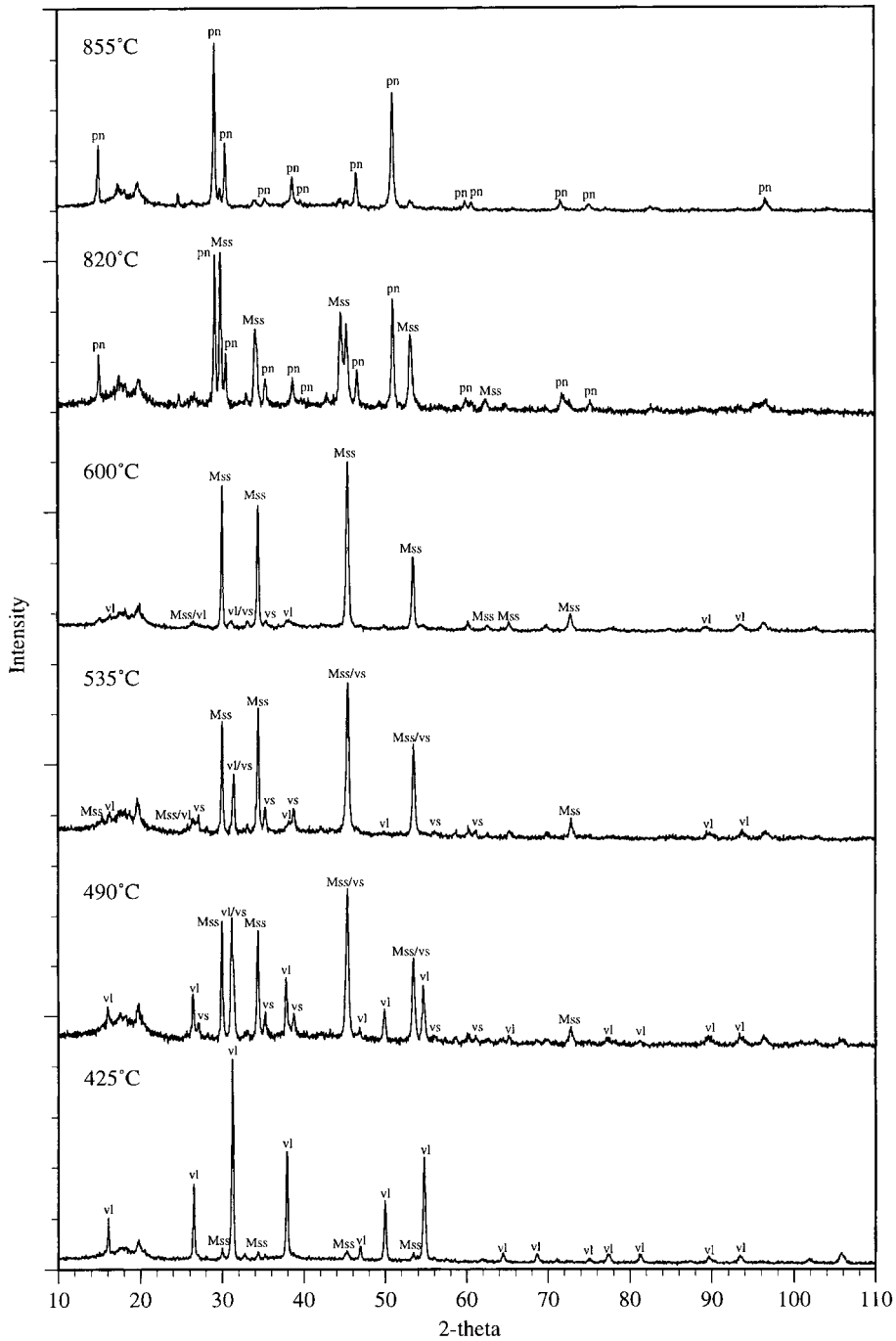


Fig. 2. XRD patterns for $\text{Fe}_{0.97}\text{Ni}_{1.96}\text{S}_4$ heated at $10^\circ\text{C min}^{-1}$ in a nitrogen atmosphere. Samples were collected at selected temperatures for analysis. The temperature and phases identified are indicated on each pattern. (vl, violarite; mss, monosulphide solid solution; vs, vaesite; and pn, pentlandite).

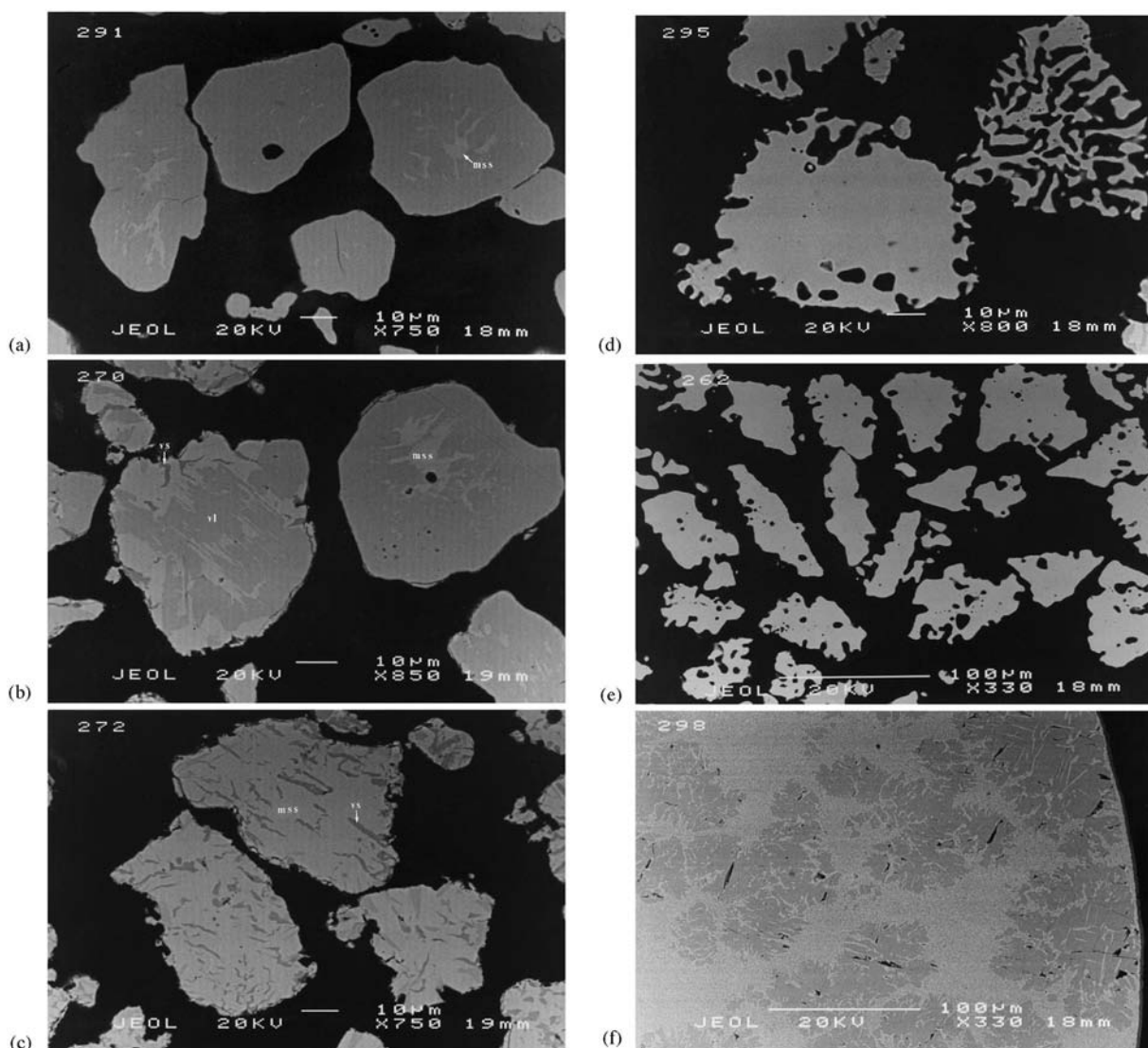


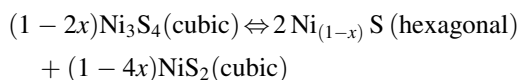
Fig. 3. BSE micrographs of $\text{Fe}_{0.97}\text{Ni}_{1.96}\text{S}_4$ collected at various temperatures (a) 425°C: Note mss phase (light grey) in the unreacted violarite (dark grey) host. (b) 490°C: violarite, major phase; mss exsolved within the violarite host; minor phase, vaesite, detected in the particle on the left as the small dark grey phase in the mss. (c) 535°C: Major phases mss (defect NiAs structure) and vaesite (cubic disulphide phase). (d) 600°C: Major phase mss. Large macropores are evident in a number of the particles. (e) 795°C: Partial melting of the mss can be observed with a number of the macropores collapsed forming holes within the mss particle. (f) 870°C: Major phases, pentlandite and mss. The thin crystals of pentlandite have recrystallised along the (0001) plane of the mss.

of 495°C and 525°C, respectively. This was unlikely to be associated with the gradual mass loss observed in the TG trace, due to the intensity of the peak and the small temperature range over which the peak occurred compared with the temperature range of the mass loss. A fresh sample was heated 10°C past the offset

temperature of the endothermic peak and allowed to cool at $10^\circ\text{C min}^{-1}$. During cooling, an exothermic peak of similar intensity was observed between 495° and 465°C. This is characteristic of a reversible phase transition. Analysis by XRD of the pyrolysis product collected at 535°C showed that violarite had comple-

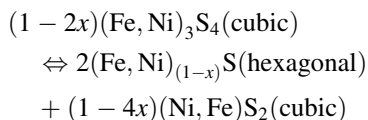
tely decomposed with mss and vaesite as the major products (Fig. 2). SEM examination showed mss as the major phase with thin dark regions of vaesite within the mss grains (Fig. 3(c)). The mean composition of the vaesite phase was $\text{Ni}_{0.83}\text{Fe}_{0.17}\text{S}_{1.85}$, similar to the ideal stoichiometry of $(\text{Ni,Fe})\text{S}_2$. The metal : sulphur ratio for the mss had increased slightly with an average composition of $\text{Fe}_{0.38}\text{Ni}_{0.55}\text{S}_{1.00}$.

Albers and Rooymans [7] reported daubreelite (FeCr_2S_4), which has a spinel structure similar to violarite, underwent a first-order phase transition at high temperatures and pressures to a hexagonal nickel-arsenide-type crystal structure. The transition was later confirmed by Bouchard [8]. By analogy, Kullerud [9] suggested that other sulphides such as polydymite and violarite may also undergo such a transformation to defect NiAs structures at elevated pressures and temperatures forming a mixture of monosulphide and disulphide. During an earlier investigation on the Ni–S system, it was reported that the decomposition of polydymite occurred at 356°C [5]. The decomposition was described by the following reaction:



Similar results were found for linnaeite, Co_3S_4 , which, when heated $>664^\circ\text{C}$, decomposed to hexagonal Co_{1-x}S and cubic CoS_2 .

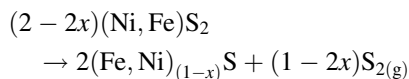
Since polydymite is the end member of the violarite solid solution, one would expect that violarite with varying iron : nickel ratios would behave similarly. Therefore, the phase transition shown in the DTA curve occurring between 495° and 525°C can be attributed to the pyrolytic decomposition of violarite to mss and vaesite according to the following reaction:



The proposed mechanism for the pyrolytic decomposition of violarite between 420° and 525°C is supported by the series of Fe–Ni–S isothermal sections shown in Fig. 4. Between 300° and 400°C , the Fe–Ni–S phase diagram shows a decrease in the violarite stability field with univariant regions formed between violarite, mss and ferroan vaesite $(\text{Ni,Fe})\text{S}_2$ or violar-

ite, mss and nickeloan pyrite $(\text{Fe,Ni})\text{S}_2$. The nickel-rich end of the stability field decreases more rapidly than the ideal stoichiometric end of the violarite solid solution. As sulphur is evolved from the violarite sample between 420° and 525°C , the composition falls below the ideal metal : sulphur ratio of 3 : 4. This shift in the composition of the sulphide below the violarite stability field results in the exsolution of mss within the violarite host. Analysis of the violarite and mss showed there was a shift in the iron : nickel ratio towards the iron boundary of the Fe–Ni–S ternary phase diagram. The decrease in nickel from the violarite and mss can be accounted for by the formation of vaesite. Therefore, the bulk composition of the violarite sample must lie within the expanding univariant region formed between violarite, mss and vaesite. Between 450° and 500°C , the ternary phase diagram shows violarite decomposes to form a divariant region between mss and vaesite. The decomposition of the violarite commenced at 495°C . This was $\approx 35^\circ\text{C}$ higher than the maximum thermal stability temperature previously reported [10] for synthetic violarite using evacuated silica tube experiments. The difference in the decomposition temperature of violarite can be attributed to the different experimental conditions used. By 525°C , the violarite has completely decomposed to mss and vaesite.

Between 525° and 615°C , the rate of mass loss increased, with a loss of 7.65% observed. The mass loss coincided with a broad endotherm which occurred in the 560 – 625°C range. The XRD pattern showed mss as the major phase with only a very minor trace of violarite remaining after 600°C (Fig. 2). No vaesite was evident in the XRD pattern. The minor trace of violarite was probably formed during the cooling stage of the pyrolysis product due to the reversible reaction between mss and the remaining vaesite. Micrographs of samples collected at 600°C showed the outer rim of the sulphide particle to be quite irregular in shape with a porous structure (Fig. 3(d)). Large macropores were evident in a number of particles. The formation of the pores was probably due to the rapid evolution of sulphur caused by high internal pressures from within the sulphide particle as the vaesite decomposed to mss according to the following equation:



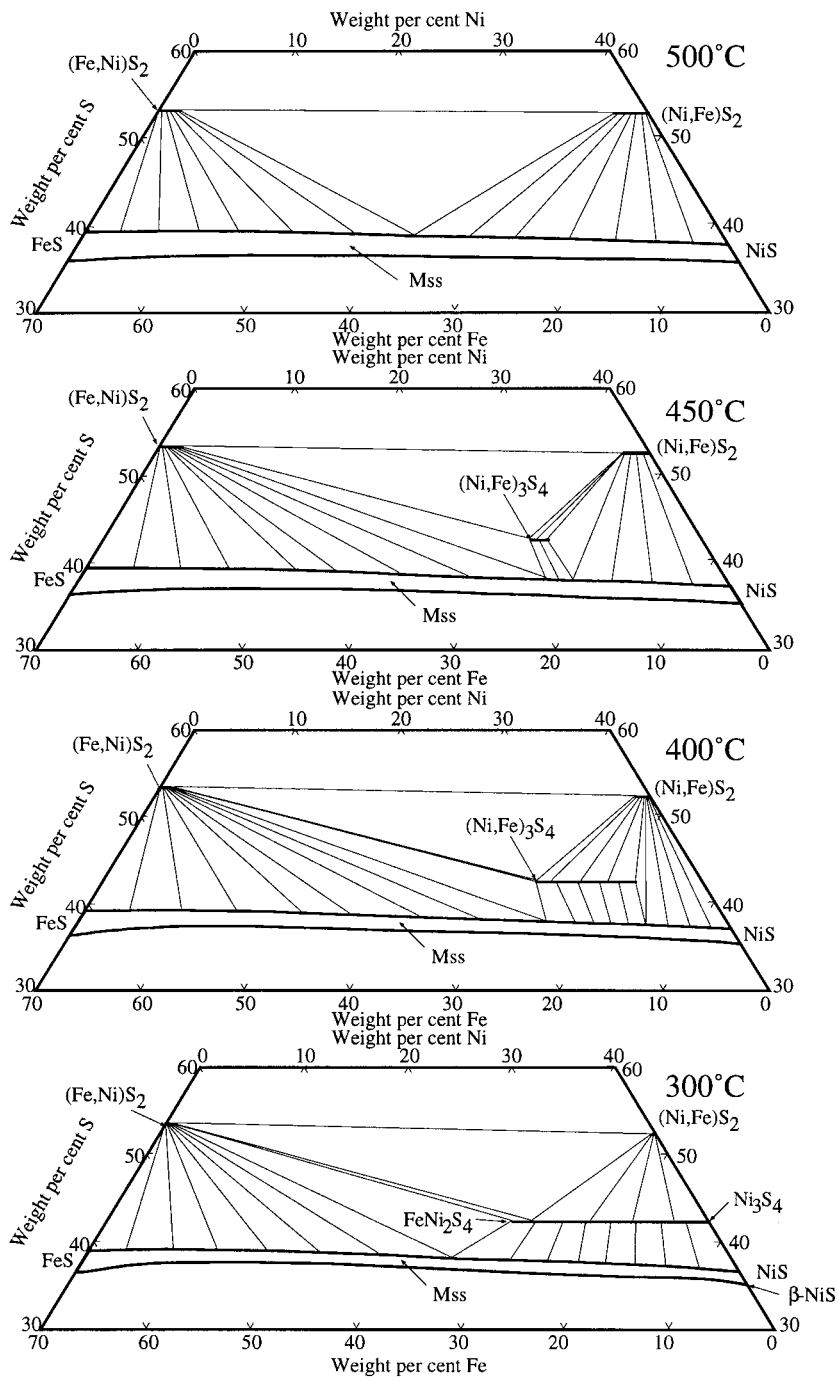


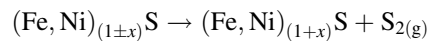
Fig. 4. Fe–Ni–S ternary phase diagram illustrating the thermal stability of the violarite–polydymite solid solution at: 500°, 450°, 400° and 300°C (Redrawn from Craig [10]).

An increase in the surface area of the sulphide particles can be clearly seen from the micrographs after the decomposition of violarite. Analysis of a number of mss particles by EPMA showed that they were homogeneous with a mean composition of $\text{Fe}_{0.36}\text{Ni}_{0.59}\text{S}_{1.00}$. The composition of the mss was in close agreement with the theoretical composition of $\text{Fe}_{0.31}\text{Ni}_{0.64}\text{S}_{1.00}$, calculated from the mass loss from the TG curve observed between 420° and 625°C.

Between 615° and 845°C, a gradual mass loss of 4.10% was observed. This mass loss was associated with a slight endothermic drift in the DTA baseline commencing at 620°C. Pyrolysis products collected at 725°C and examined by SEM revealed a homogeneous mss phase. By 795°C, the mss phase exhibited partial melting (see Fig. 3(e)). The surfaces of the particles were relatively smooth compared to those particles collected at 600°C (Fig. 3(d)). A number of the macropores had collapsed, leaving small gaseous

inclusions in the sulphide particles. EPMA analysis of the mss phase collected at 725°C and 795°C showed a loss of sulphur with average compositions of $\text{Fe}_{0.36}\text{Ni}_{0.66}\text{S}_{1.00}$ and $\text{Fe}_{0.37}\text{Ni}_{0.74}\text{S}_{1.00}$ at the respective temperatures. A minor trace of pentlandite was also detected within some mss particles collected at 795°C, appearing as a brighter phase when compared with the mss phase.

Hence, the gradual mass loss between 615° and 795°C can be associated with the continual loss of sulphur from the mss phase.



The reaction sequence between 615° and 795°C can be explained by a series of Fe–Ni–S ternary phase diagrams. Fig. 5 shows an isothermal section at 650°C from the Fe–Ni–S ternary phase system. At 650°C, mss and $(\text{Fe, Ni})_{(3\pm x)}\text{S}_2$ may coexist in equilibrium with each other. A central sulphide liquid region

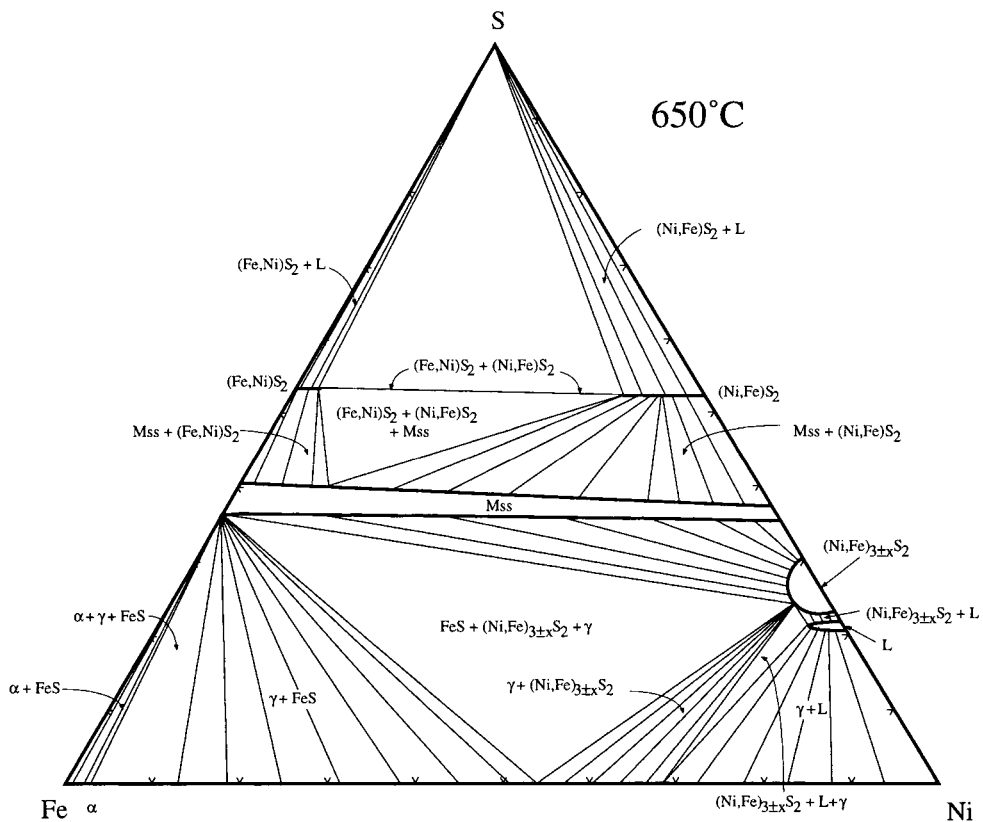
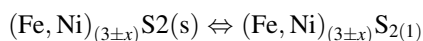


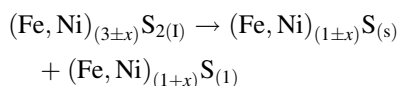
Fig. 5. Fe–Ni–S phase diagram at 650°C (redrawn from Kullerud [12]). All phases and assemblages coexist with sulphur vapour.

appears at 635°C and forms a divariant region with $(\text{Fe,Ni})_{(3\pm x)}\text{S}_2$. By 860°C, the central sulphide liquid region expands considerably with a univariant region formed between mss and $(\text{Fe,Ni})_{(3\pm x)}\text{S}_2$, and a divariant region with $(\text{Fe,Ni})_{(3\pm x)}\text{S}_2$ (see Fig. 6). Between 615° and 795°C, the mss stability field expands vertically, allowing the metal : sulphur ratio to increase resulting in the loss of sulphur. Analysis of the mss between 725° and 795°C showed that the metal : sulphur ratio increased from 1.02 to 1.11. According to the ternary phase diagram shown in Fig. 6, the composition of the mss falls below the mss stability field in this temperature range, resulting in the formation of a high-temperature haezlewoodite phase, $(\text{Fe,Ni})_{3\pm x}\text{S}_2$, coexisting in equilibrium with mss.

The presence of the high-temperature $(\text{Fe,Ni})_{(3\pm x)}\text{S}_2$ phase was confirmed by a sharp endotherm with an onset temperature of 835°C, observed in the DTA trace. This corresponded to the incongruent melting point of $(\text{Fe,Ni})_{(3\pm x)}\text{S}_2$ to mss and the central sulphide liquid phase [11]. Kullerud and Yund [5] reported the melting point of a ternary phase with a metal : sulphur composition of nearly 3 : 2, $\text{Ni}_{3\pm x}\text{S}_2$, similar to haezlewoodite, to be 806°C:



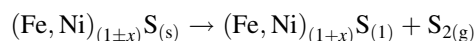
and



XRD results obtained from a sample collected at 820°C, coinciding with the melting point transition, detected mss and pentlandite present. The high-temperature $(\text{Fe,Ni})_{(3\pm x)}\text{S}_2$ phase is a non-quenchable phase. On cooling, the central sulphide liquid will react with mss to form $(\text{Fe,Ni})_{(3\pm x)}\text{S}_2$ at 862°C [12]. Between 862° and 610°C, the mss and $(\text{Fe,Ni})_{(3\pm x)}\text{S}_2$ assemblage remains stable. Below 610°C, pentlandite is formed by the reaction between mss and $(\text{Fe,Ni})_{(3\pm x)}\text{S}_2$ [12] [13]. Therefore, any central sulphide liquid or $(\text{Fe,Ni})_{(3\pm x)}\text{S}_2$ present during the cooling of the pyrolysis product will completely react to form pentlandite with excess mss remaining. By 855°C, there was only slight evidence of mss present with pentlandite as the major phase.

A broad endotherm followed the melting point transition with onset and offset temperatures of

845° and 900°C, respectively. A mass loss of 4.85% coincided with the endotherm. This was associated with the continual loss of sulphur from the mss phase to form additional central sulphide liquid phase:



By 890°C, the sulphide was completely molten, forming a spherical metal sulphide bead during quenching of the sample. BSE micrographs of the molten product quenched at 870°C (Fig. 4(f)) showed preferred orientation of pentlandite along the mss during recrystallisation. The exsolved pentlandite formed thin coherent needles with either the (111) pentlandite plane parallel to the (0001) mss plane or (110) pentlandite plane parallel to the (1010) mss plane [14]. Rapidly quenched samples of $(\text{Fe,Ni})_{(1-x)}\text{S}$ solid solutions showed that the pentlandite recrystallised in randomly oriented blebs due to the planes of exsolved pentlandite not aligning with the mss lattice.

The average composition of the pentlandite phase collected at 890°C was $\text{Fe}_{3.11}\text{Ni}_{6.00}\text{S}_8$. The composition is in agreement with the general formula of pentlandite, $(\text{Fe,Ni})_9\text{S}_8$, with the Fe : Ni ratio corresponding to the initial violarite composition. The TG curve showed a continued loss of mass up to 1000°C with no DTA activity. A total loss of 21.45% was observed from ambient temperature to 1000°C. The calculated composition from the observed mass loss falls within the central sulphide-phase stability field of the Fe–Ni–S ternary phase diagram at 1000°C.

3.1. Effect of stoichiometry on the pyrolytic decomposition of synthetic violarite

Thermal analysis was performed on the four violarite samples to determine the effect of stoichiometry on the mechanism of pyrolytic decomposition. The TG-DTA traces for each synthetic violarite are presented in Fig. 7. The extrapolated onset and offset temperatures for each endothermic event are tabulated in Table 2. The reaction mechanism for the decomposition of synthetic violarite was not affected by a change in the iron : nickel ratio. However, there were significant shifts in the onset and offset temperatures for the TG-DTA events as the iron : nickel ratio tended towards the nickel rich end member of the violarite series. The intensity and range of the endothermic

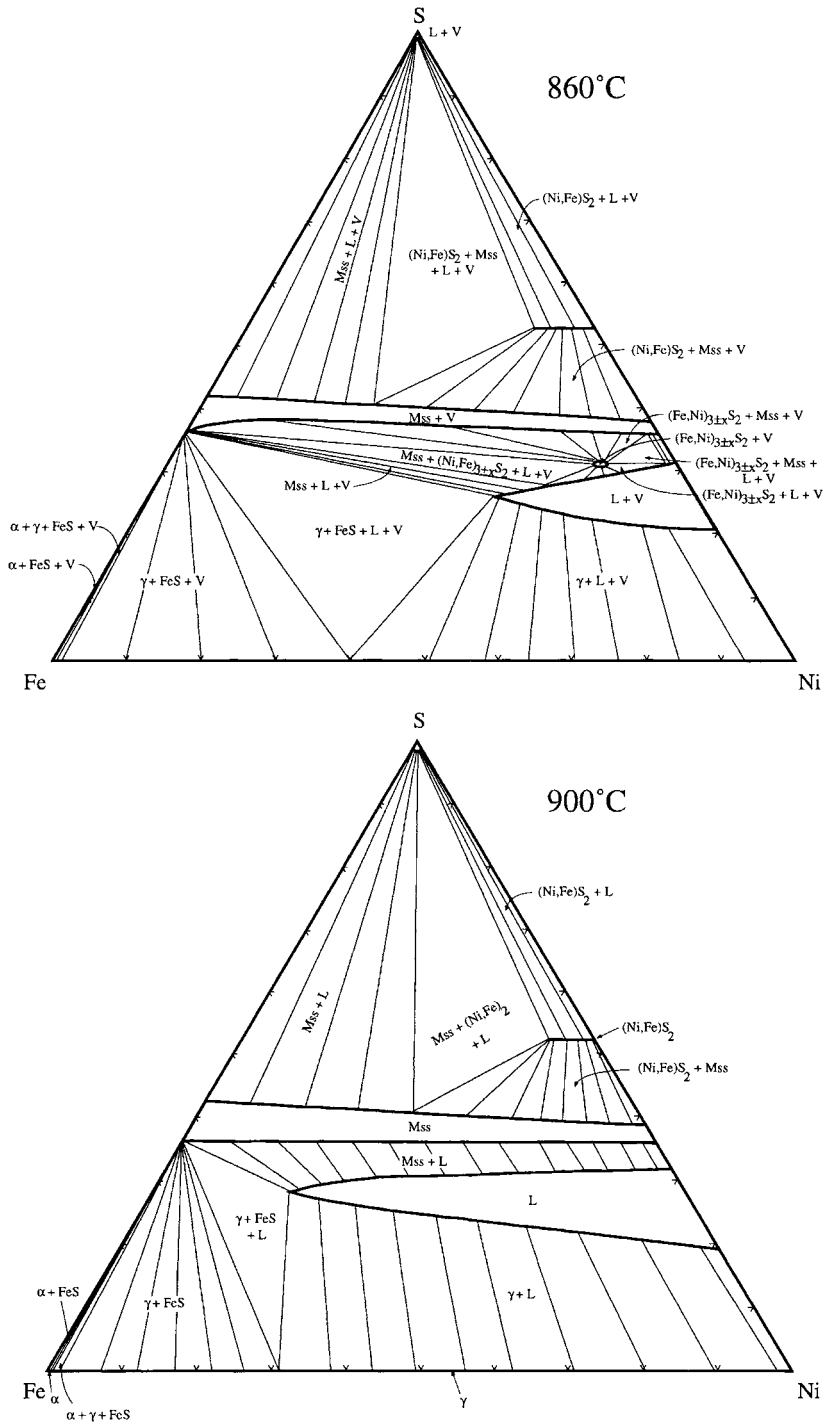


Fig. 6. Fe–Ni–S phase diagram at 860° and 900°C (redrawn from Kullerud [12]). All phases and assemblages coexist with sulphur vapour.

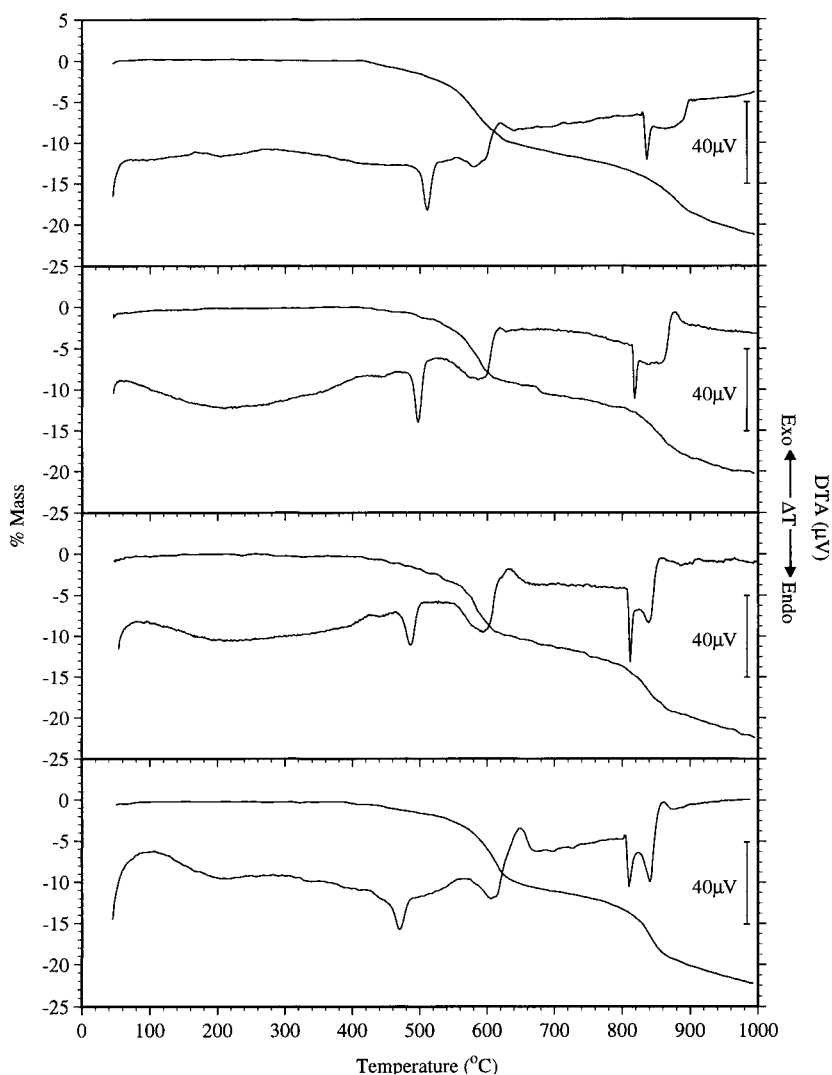


Fig. 7. Typical TG-DTA traces for the four violarites, heated at $10^{\circ}\text{C min}^{-1}$ in a nitrogen atmosphere. Starting from the top $\text{Fe}_{0.97}\text{Ni}_{1.96}\text{S}_4$, $\text{Fe}_{0.73}\text{Ni}_{2.26}\text{S}_4$, $\text{Fe}_{0.46}\text{Ni}_{2.49}\text{S}_4$, and $\text{Fe}_{0.20}\text{Ni}_{2.72}\text{S}_4$.

peaks also showed minor variations with the stoichiometry of the violarite.

The onset temperature for the initial endotherm associated with the incongruent phase transition of violarite to mss and vaesite showed a significant decrease as the iron : nickel ratio decreased. The pyrolytic decomposition temperature of synthetic violarite was characterised earlier by the onset temperature of the phase transition of violarite to mss and vaesite. Fig. 8 shows the effect of stoichiometry of

synthetic violarite on the pyrolytic decomposition temperature, which decreases linearly as the iron : nickel ratio decreases. Thus, the onset temperature decreased from 495° to 450°C as the iron : nickel ratio decreased from 0.49 to 0.07. The pyrolytic decomposition temperature of synthetic violarite heated at $10^{\circ}\text{C min}^{-1}$ in nitrogen can be described by the equation derived from line of least-squares of $\text{Temp} (^{\circ}\text{C}) = 107.7(\text{Fe} : \text{Ni ratio}) + 445.9$ with a correlation coefficient of 0.99.

Table 2

Comparison of the extrapolated onset and offset temperatures for the major endothermic activity for a range of synthetic violarites under pyrolytic decomposition conditions of $10^{\circ}\text{C min}^{-1}$ in a nitrogen atmosphere using TG-DTA

Sulphide	Temperature of endothermic events ($^{\circ}\text{C}$)			
	phase transition from thiospinel \rightarrow mss (defect NiAs structure) + vaesite	decomposition of vaesite to mss	incongruent melting point transition of high temperature $(\text{Fe,Ni})_{3\pm x}\text{S}_2$	evolution of sulphur from central liquid phase
$\text{Fe}_{0.97}\text{Ni}_{1.96}\text{S}_4$	495–525	560–625	835–845	845–900
$\text{Fe}_{0.73}\text{Ni}_{2.26}\text{S}_4$	485–510	545–615	815–825	825–870
$\text{Fe}_{0.46}\text{Ni}_{2.49}\text{S}_4$	470–500	550–620	810–820	825–850
$\text{Fe}_{0.20}\text{Ni}_{2.72}\text{S}_4$	450–485	575–650	805–825	825–855

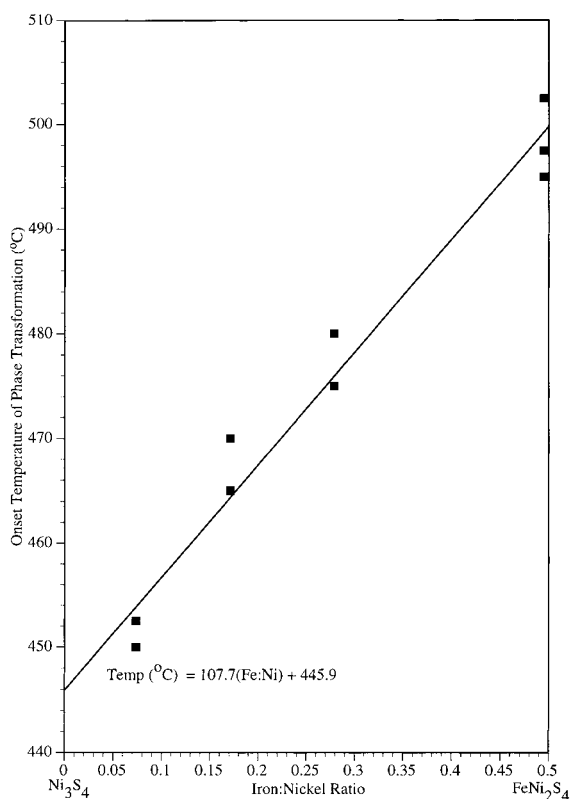


Fig. 8. The effect of composition on the pyrolytic decomposition of synthetic violarite characterised by the phase transformation of spinel crystal structure \rightarrow defect NiAs structure and disulphide. Each sulphide was analysed in triplicate (some points may overlap).

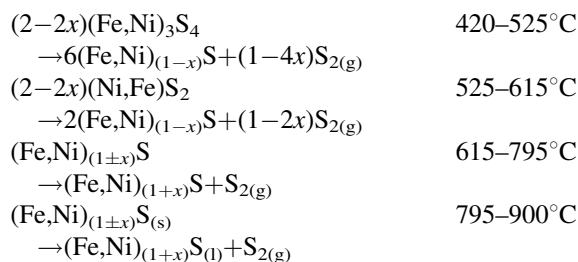
The onset temperature of the broad endothermic peak associated with the decomposition of vaesite remained constant for all four violarite samples.

The incongruent melting point of $(\text{Fe,Ni})_{(3\pm x)}\text{S}_2$ showed a decrease from 830° to 805°C as the iron : nickel ratio decreased. DTA experiments performed by Kullerud in sealed silica tubes reported a 56°C increase in the melting point from 806° to 862°C , between $\text{Ni}_{(3\pm x)}\text{S}_2$ and an iron-saturated $(\text{Fe,Ni})_{(3\pm x)}\text{S}_2$ phase [11].

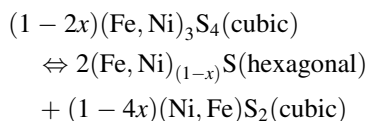
The incongruent melting point transition was immediately followed by another broader endotherm. The temperature range in which the endothermic peak was observed decreased as the iron : nickel ratio decreased. The mass loss coinciding with the endotherm increased as the iron : nickel ratio decreased, with losses of 4.85% ($845\text{--}900^{\circ}\text{C}$) and 6.10% ($815\text{--}865^{\circ}\text{C}$) observed for $\text{Fe}_{0.97}\text{Ni}_{1.96}\text{S}_4$ and $\text{Fe}_{0.20}\text{Ni}_{2.72}\text{S}_4$. Total mass losses of 21.50 and 22.55%, respectively, were observed for the two violarites between $25\text{--}1000^{\circ}\text{C}$.

4. Conclusions

The reaction sequence for the pyrolytic decomposition of violarite consisted of a series of reactions in which sulphur was progressively eliminated:



The endotherm at 495°C associated with no mass loss was attributed to an incongruent phase transition as described by the equation:



A further endotherm at 835°C was caused by the melting of a high temperature form of heazlewoodite with a general formula of $(\text{Fe, Ni})_{(3\pm x)}\text{S}_2$. The temperatures of both endotherms decreased as the content of nickel in the original violarite sample increased.

References

- [1] E.H. Nickel, J.R. Ross, M.E. Thornber, *Econ. Geol.* 69 (1974) 93–107.
- [2] K.C. Misra, M.E. Fleet, *Econ. Geol.* 69 (1974) 391–403.
- [3] G.A. Desborough, G.K. Czamanske, *Amer. Miner.* 58 (1973) 195–202.
- [4] D.R. Hudson, D.I. Groves, *Econ. Geol.* 69 (1974) 1335–1340.
- [5] G. Kullerud, R.A. Yund, *J. Petrology* 3(1) (1962) 126–175.
- [6] D.J. Vaughan, J.R. Craig, *Mineral Chemistry of Metal Sulphides*, Cambridge University Press, London, 1978, pp. 267.
- [7] W. Albers, C.J.M. Rooymans, *Solid State Comms.* 3 (1965) 417–419.
- [8] R.J. Bouchard, *Mater. Res. Bul.* 2 (1967) 459–464.
- [9] G. Kullerud, *Carnegie Institute of Washington Annual Report* 67 (1968) 179–182.
- [10] J.R. Craig, *Amer. Miner.* 56 (1971) 1303–1311.
- [11] G. Kullerud, *Canad. Miner.* 7(1) (1962) 353–366.
- [12] G. Kullerud, *Carnegie Institute of Washington Annual Report* 62 (1962) 175–189.
- [13] W.E. Ewers, *Proc. Austral. Inst. Min. Metall.* 241 (1973) 19–26.
- [14] C.A. Francis, M.E. Fleet, K. Misra, J.R. Craig, *Amer. Miner.* 61 (1976) 913–920.